Automatica 48 (2012) 505–513

Contents lists available at SciVerse ScienceDirect

Automatica

journal homepage: www.elsevier.com/locate/automatica

Brief paper

State-space solution to weight optimization problem in $\mathscr{H}_\infty$ loop-shaping control☆

M. Osinuga [a,1], S. Patra [b], A. Lanzon [a]

[a] Control Systems Centre, School of Electrical and Electronic Engineering, University of Manchester, Sackville Street, Manchester, M13 9PL, United Kingdom

[b] Department of Electrical Engineering, Indian Institute of Technology, Kharagpur, 721302, India

ARTICLE INFO

Article history:
Received 2 September 2010
Received in revised form
27 May 2011
Accepted 31 July 2011
Available online 13 January 2012

Keywords:
$\mathscr{H}_\infty$ loop-shaping
Robust stability margin
Weight optimization
Convex optimization

ABSTRACT

This paper proposes a state-space solution to weight optimization problem in $\mathscr{H}_\infty$ loop-shaping control. A pointwise-in-frequency weight optimization framework is transformed into convex optimization searches that are independent of frequency. The introduced optimization problem therefore avoids gridding of the frequency space and consequently, the inaccuracies attributed to fitting transfer functions to magnitude data. In this optimization problem, the order of the weight is specified 'a priori', thus facilitating the synthesis of low-order controllers, which is desirable from an implementation perspective. The proposed solution algorithm simultaneously synthesizes a robust stabilizing controller and a loop-shaping weight (pre-compensator) that maximize the robust stability margin subject to constraints on the performance and the singular values of the weight. Three numerical examples are given to illustrate the effectiveness of the technique.

1. Introduction

The $\mathscr{H}_\infty$ loop-shaping design procedure (LSDP), proposed by McFarlane and Glover (1992), is a simple and efficient robust multi-input multi-output (MIMO) controller synthesis technique that combines classical loop-shaping concepts with $\mathscr{H}_\infty$ synthesis. This well-known design procedure establishes a good tradeoff between robust stability and robust performance of a closed-loop system. Fig. 1 shows this design framework where a stabilizing controller C_∞ is synthesized for the shaped plant $P_s = W_2PW_1$ and the final $\mathscr{H}_\infty$ loop-shaping controller is obtained by cascading weights with the stabilizing controller C_∞ as $\mathbf{C} = W_1C_\infty W_2$. Typically, $\mathbf{C}$ is of order $n_p + 2n_w$ (McFarlane & Glover, 1990), where n_p is the order of P and n_w is the combined orders of W_1 and W_2. This implies that low-order weights facilitate the synthesis of low-order controllers.

In this design procedure, loop-shaping weights W_1 and W_2 are used to shape the singular values of the nominal plant based on the closed-loop performance specifications, and a stabilizing controller that maximizes the robust stability margin is thereafter synthesized. However, weight selection is non-trivial especially for plants with strong coupling (Hyde, 1995; Lanzon, 2001, 2005; McFarlane & Glover, 1992; Papageorgiou & Glover, 1997; Tsai, Geddes, & Postlethwaite, 1990); factors such as the right-half plane (RHP) poles/zeros of the nominal plant, roll-off rate around crossover, expected bandwidth, singular values and condition numbers of the nominal plant, etc. must also be duly considered. In Lanzon (2001, 2005), these factors have been captured within an optimization framework that maximizes the robust stability margin for a given performance. The solution to the resulting optimization problem simultaneously synthesizes weights and a stabilizing controller.

Although this optimization problem is formulated to hold on a continuum of frequencies, i.e., infinite number of constraints due to the dependence on frequency, it can only be solved by gridding the frequency space. The difficulty in gridding increases with the 'non-smoothness' in the variations of the magnitude response of the plant since the number of grid-points must be chosen such that the intrinsic properties of the plant and the required performance are adequately captured. Furthermore, transfer functions are fitted to the magnitude data obtained from the solution of the pointwise-in-frequency optimization problem to form the loop-shaping weights at each iteration. While high-order transfer functions are required to obtain good curve-fitting for some magnitude data, precise fitting is infeasible in some other cases irrespective of the order of the transfer function, and this might often result in the violation of some of the design constraints. This is due to the fact that curve-fitting depends also on the magnitude response of the plant, in view of the performance requirements. Moreover, fitting, which

☆ The financial support of the Engineering and Physical Sciences Research Council and the Royal Society is gratefully acknowledged. This paper was not presented at any IFAC meeting. This paper was recommended for publication in revised form by Associate Editor Tong Zhou under the direction of Editor Roberto Tempo.

E-mail addresses: mobolaji.osinuga-2@postgrad.manchester.ac.uk (M. Osinuga), sourav@ee.iitkgp.ernet.in (S. Patra), alexander.lanzon@manchester.ac.uk (A. Lanzon).

[1] Tel.: +44 161 306 28 21; fax: +44 161 306 93 41.

0005-1098/$ – see front matter © 2011 Elsevier Ltd. All rights reserved.
doi:10.1016/j.automatica.2011.11.008

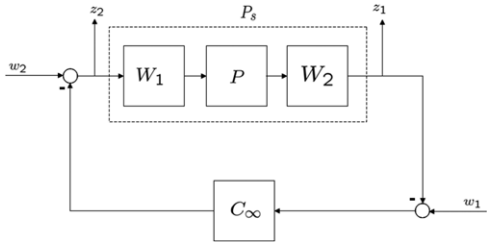

Fig. 1. $\mathscr{H}_\infty$ loop-shaping design framework.

affects the rate and point of convergence of the solution algorithm, requires a lot of memory allocation when there are many grid-points.

In this paper, the frequency-dependent optimization problem in Lanzon (2005) is transformed to convex optimization searches that are independent of frequency, thereby circumventing the problems associated with frequency gridding and transfer function fitting. The resulting solution algorithm maximizes the robust stability margin over a fixed-order (chosen 'a priori') diagonal weight subject to constraints which ensure that the loop-shape and the singular values/condition number of the weight lie in pre-specified regions. Since it is not a requirement that the specification of the loop-shaping weights be left entirely up to the optimization procedure, corresponding weights, if known to achieve certain level of performance and/or robustness, can be absorbed into the plant. The optimization-based synthesis can then be thought of as a systematic mechanism for 'tuning' the specified weights, and hence, the overall design. The post-compensator, fixed as the identity in the formulation, can similarly be cascaded with the nominal plant (as a low-pass filter usually), if required.

The rest of the paper is organized as follows. Notations are defined in Section 2 while the optimization problem of Lanzon (2005), stated in Section 3, is reformulated using the state-space approach in Section 4. In this section, a fixed-order pre-compensator is parameterized and incorporated in the frequency-dependent optimization framework in such a way that the convexity of the optimization problem is retained. The KYP lemma (Rantzer, 1996) is then invoked on the new formulation to remove the dependency on frequency. The resulting solution algorithm, three illustrative examples and the conclusions are given in Sections 5–7, respectively.

2. Notations

Let $\mathbb{R}$ and $\mathbb{R}_+$ denote the set of real and strictly positive real numbers, respectively. Let $\mathscr{L}_\infty$ denote the space of functions bounded on $j\mathbb{R}$, including ∞, and let $\mathscr{H}_\infty$ denote the subspace of functions in $\mathscr{L}_\infty$ that are bounded and analytical in the open RHP. Moreover, let prefix $\mathscr{R}$ denote the proper real-rational subspaces of the above function spaces. Functions that are units in $\mathscr{RH}_\infty$ are said to belong to $\mathscr{GH}_\infty$, i.e., $f \in \mathscr{GH}_\infty \Leftrightarrow f, f^{-1} \in \mathscr{RH}_\infty$. The i-th singular value of matrix A is represented as $\sigma_i(A)$ and the condition number is defined as $\kappa(A) := \overline{\sigma}(A)/\underline{\sigma}(A)$, where $\overline{\sigma}(A)$ (resp. $\underline{\sigma}(A)$) is the largest (resp. smallest) singular value of matrix A. A^T and A^* are the transpose and complex conjugate transpose of matrix A, respectively. While the dimension of the identity matrix is omitted when it is clear from the context, the $n \times n$ identity matrix is denoted by I_n. $X \otimes Y$ is the Kronecker product of X and Y and $\mathrm{diag}\begin{pmatrix} a \\ b \end{pmatrix}$ is a shorthand notation for $\begin{pmatrix} a & 0 \\ 0 & b \end{pmatrix}$.

Let the feedback interconnection of P_s and C_∞ shown in Fig. 1 be denoted by $[P_s, C_\infty]$. Also, denote by $\mathscr{C}(P_s)$ the set of all stabilizing controllers for P_s, i.e. $\mathscr{C}(P_s) := \{C_\infty : [P_s, C_\infty] \text{ is internally stable}\}$. Then, the robust stability margin of $[P_s, C_\infty]$ is defined as

$$b(P_s, C_\infty) := \left\| \begin{bmatrix} P_s \\ I \end{bmatrix} (I - C_\infty P_s)^{-1} \begin{bmatrix} -C_\infty & I \end{bmatrix} \right\|_\infty^{-1} \tag{1}$$

if $C_\infty \in \mathscr{C}(P_s)$ or otherwise 0. The maximum achievable robust stability margin is $b_{opt}(P_s) := \sup_{C_\infty} b(P_s, C_\infty) \in [0, 1]$ (Glover & McFarlane, 1989). The McMillan degree of a transfer function matrix $G(s)$ with a minimal state-space realization (A_i, B_i, C_i, D_i) is denoted by n_i, where i is a positive integer.

3. Pointwise-in-frequency weight optimization problem

The robust stability margin indicates the size of the largest $\mathscr{H}_\infty$ ($\mathscr{L}_\infty$)-norm bounded perturbation of the normalized coprime factors of $P_s = W_2 P W_1$ for which closed-loop stability is guaranteed (McFarlane & Glover, 1990; Vinnicombe, 2001, Theorem 1.20). It also shows the compatibility of the performance specifications with the achieved loop-shape. Moreover, the upper bounds of the standard closed-loop design objectives, discussed in McFarlane and Glover (1992) and Zhou, Doyle, and Glover (1996, Theorem 18.11), are specified as function of the shaped plant, the robust stability margin and the singular values and condition numbers of the weights. A designer must ensure that the gain of these objectives are made small in particular frequency regions.

Consequently, the optimization problem in Lanzon (2005) is formulated to maximize the robust stability margin over loop-shaping weights, subject to constraints that ensure satisfactory loop-shape, singular values and condition numbers of the synthesized weights as follows.

For a scaled plant $P \in \mathscr{RL}_\infty^{m\times n}$, where $m \geq n$,

$$\max_{\substack{W_1 \in \mathscr{GH}_\infty \\ W_2 \in \mathscr{GH}_\infty}} b_{opt}(W_2 P W_1)$$

subject to

$$|\underline{s}(j\omega)| < \sigma_l(P_s(j\omega)) < |\overline{s}(j\omega)| \quad \forall l, \omega, \tag{2a}$$

$$|\underline{w}_1(j\omega)| < \sigma_l(W_1(j\omega)) < |\overline{w}_1(j\omega)|,$$

$$|\underline{w}_2(j\omega)| < \sigma_l(W_2(j\omega)) < |\overline{w}_2(j\omega)| \quad \forall l, \omega, \tag{2b}$$

$$\kappa(W_1(j\omega)) < |k_1(j\omega)|, \qquad \kappa(W_2(j\omega)) < |k_2(j\omega)| \quad \forall \omega, \tag{2c}$$

where $|\underline{s}(j\omega)|$ and $|\overline{s}(j\omega)|$, specified based on the closed-loop performance requirements, are boundaries for an allowable loop-shape, $|\underline{w}_i(j\omega)|$ and $|\overline{w}_i(j\omega)|$ delimit the allowable region for the singular values of loop-shaping weight $W_i(j\omega)$ $(i = 1, 2)$ and $|k_i(j\omega)|$ provides bounds for the condition number of loop-shaping weight $W_i(j\omega)$ $(i = 1, 2)$. The assumption that the plant has more outputs than inputs incurs no loss of generality; a dual problem to that shown in Fig. 1 where $W_1 = W_2^T, W_2 = W_1^T, P = P^T$ and $C_\infty = C_\infty^T$ would be considered if the plant has strictly fewer outputs than inputs.

Using the definition of $b(P_s, C_\infty)$ given in (1) and performing several algebraic manipulations, this problem was formulated into a frequency-dependent quasiconvex optimization problem. The solution algorithm thus requires gridding of the frequency space, which should of necessity capture the plant's dynamics and the performance specifications. When the frequency space is gridded to solve the optimization problem, there arises a difficulty in fitting[2] transfer functions to the obtained magnitude data (see Fig. 3 for instance, where the plant is lightly-damped). Moreover, curve-fitting often yields high-order transfer functions, depending on the 'complexities' involved.

4. Proposed frequency-independent weight optimization framework

In order to circumvent the aforementioned problems while still satisfying the design objectives, the state-space equivalence of the optimization problem stated in the previous section is now formulated. In this formulation, the post-compensator W_2

[2] Although perfect weighting function is desirable, a good approximation is often sufficient in practice.

is fixed as the identity and the optimization is over a diagonal pre-compensator W_1, which is in line with the observation that diagonal loop-shaping weights are generally sufficient to shape the singular values of the nominal plant (Hyde, 1995). The structure and the order of W_1 are specified 'a priori' using a parametrization (Sandberg, Lanzon, & Anderson, 2006a,b) which we define next.

4.1. Parametrization of the diagonal pre-compensator

With the aim of formulating a tractable frequency-independent problem, a p-th order pre-compensator $W_1 \in \mathscr{GH}_\infty^{n\times n}$ is parameterized as follows:

$$W_1(s) := \left(a_p s^p + a_{p-1}s^{p-1} + \cdots + a_0\right) \times \left[\operatorname{diag}\begin{pmatrix} b_p^1 s^p + b_{p-1}^1 s^{p-1} + \cdots + b_0^1 \\ \vdots \\ b_p^n s^p + b_{p-1}^n s^{p-1} + \cdots + b_0^n \end{pmatrix}\right]^{-1},$$

where coefficients $a_i, b_i^k \in \mathbb{R}\ \forall i = 0, 1, \ldots, p, k = 1, 2, \ldots, n$.

We define $\Lambda_{1\omega}$ as follows:

$$\begin{aligned}\Lambda_{1\omega} &= W_1(j\omega)^{-*}W_1(j\omega)^{-1} \\ &= \left(\frac{1}{a_p(-j\omega)^p + a_{p-1}(-j\omega)^{p-1} + \cdots + a_0}\right) \\ &\quad \times \left(\frac{1}{a_p(j\omega)^p + a_{p-1}(j\omega)^{p-1} + \cdots + a_0}\right) \\ &\quad \times \operatorname{diag}\begin{pmatrix} b_p^1(-j\omega)^p + b_{p-1}^1(-j\omega)^{p-1} + \cdots + b_0^1 \\ \vdots \\ b_p^n(-j\omega)^p + b_{p-1}^n(-j\omega)^{p-1} + \cdots + b_0^n \end{pmatrix} \\ &\quad \times \operatorname{diag}\begin{pmatrix} b_p^1(j\omega)^p + b_{p-1}^1(j\omega)^{p-1} + \cdots + b_0^1 \\ \vdots \\ b_p^n(j\omega)^p + b_{p-1}^n(j\omega)^{p-1} + \cdots + b_0^n \end{pmatrix}.\end{aligned}$$

The above can also be represented as

$$\begin{aligned}\Lambda_{1\omega} &= \left(\frac{1}{\bar{a}_{2p}\omega^{2p} + \bar{a}_{2p-2}\omega^{2p-2} + \cdots + \bar{a}_0}\right) \\ &\quad \times \operatorname{diag}\begin{pmatrix} \bar{b}_{2p}^{11}\omega^{2p} + \bar{b}_{2p-2}^{11}\omega^{2p-2} + \cdots + \bar{b}_0^{11} \\ \vdots \\ \bar{b}_{2p}^{nn}\omega^{2p} + \bar{b}_{2p-2}^{nn}\omega^{2p-2} + \cdots + \bar{b}_0^{nn} \end{pmatrix},\end{aligned} \tag{3}$$

where

$$\bar{a}_{2i} := \begin{cases} a_i^2 & \text{if } i = 0, p \\ a_i^2 - \sum_{x=1}^{i} 2a_{2x-2}a_{2x} & \\ \quad + \sum_{x=1}^{i} 2a_{2x-1}a_{2x+1} & \text{if } i = 1, 2, \ldots, p-1, \end{cases}$$

$$\bar{b}_{2i}^{yy} := \begin{cases} (b_i^y)^2 & \text{if } i = 0, p \\ (b_i^y)^2 - \sum_{x=1}^{i} 2b_{2x-2}^y b_{2x}^y & \\ \quad + \sum_{x=1}^{i} 2b_{2x-1}^y b_{2x+1}^y & \text{if } i = 1, 2, \ldots, p-1, \end{cases}$$

$y = 1, 2 \ldots, n$.

Furthermore, $\Lambda_{1\omega}$ in (3) can be expressed in a simplified form as

$$\Lambda_{1\omega} = \mathbf{a}_p^{-1}(\omega^2)B_p(\omega^2),$$

where

$$\mathbf{a}_p(\omega^2) = \bar{a}_{2p}\omega^{2p} + \bar{a}_{2p-2}\omega^{2p-2} + \cdots + \bar{a}_0 \quad \text{and}$$

$$B_p(\omega^2) = \operatorname{diag}\begin{pmatrix} \bar{b}_{2p}^{11}\omega^{2p} + \bar{b}_{2p-2}^{11}\omega^{2p-2} + \cdots + \bar{b}_0^{11} \\ \vdots \\ \bar{b}_{2p}^{nn}\omega^{2p} + \bar{b}_{2p-2}^{nn}\omega^{2p-2} + \cdots + \bar{b}_0^{nn} \end{pmatrix}.$$

Note that $\mathbf{a}_p(\omega^2)$ and $B_p(\omega^2)$ are even positive scalar polynomials, where $\{\bar{a}_k\}$ and $\{\bar{b}_k^{ii}\}$, $0 \le k \le 2p$ and $1 \le i \le n$ are the unknown variables; $\mathbf{a}_p(\omega^2)$ and $B_p(\omega^2)$ have p and $p \times n$ unknown variables, respectively.

Also, defining the following in view of the state-space formulation:

$$X(s) := \begin{bmatrix} s^p \\ s^{p-1} \\ \vdots \\ 1 \end{bmatrix}, \quad \bar{A}_p := \operatorname{diag}\begin{pmatrix} \bar{a}_{2p} \\ \bar{a}_{2p-2} \\ \vdots \\ \bar{a}_0 \end{pmatrix}, \quad \bar{B}_p := \operatorname{diag}\begin{pmatrix} B_{11} \\ \vdots \\ B_{nn} \end{pmatrix},$$

where

$$B_{ii} = \operatorname{diag}\begin{pmatrix} \bar{b}_{2p}^{ii} \\ \bar{b}_{2p-2}^{ii} \\ \vdots \\ \bar{b}_0^{ii} \end{pmatrix},$$

then, the following can be written:

$$\mathbf{a}_p(\omega^2)I = (I \otimes X(j\omega))^* \left(I \otimes \bar{A}_p\right)(I \otimes X(j\omega)), \tag{4}$$

$$\begin{aligned}\mathbf{a}_p(\omega^2)P^*(j\omega)P(j\omega) &= (P(j\omega) \otimes X(j\omega))^* \\ &\quad \times \left(I_n \otimes \bar{A}_p\right)(P(j\omega) \otimes X(j\omega)),\end{aligned} \tag{5}$$

$$B_p(\omega^2) = (I_n \otimes X(j\omega))^* \bar{B}_p (I_n \otimes X(j\omega)). \tag{6}$$

4.2. State-space solution to weight optimization problem

Now, we reformulate the optimization problem stated in Section 3 using the state-space approach and, for simplicity sake, the dependence of $\mathbf{a}_p$ and B_p on ω^2 and P, $\mathbf{C}$, X, $\underline{s}$, $\bar{s}$, $\underline{w}_1$ and $\overline{w}_1$ on $j\omega$ is not shown. We assume that the plant P, stabilizing controller $\mathbf{C}$ and the transfer functions $\underline{s}(s)$, $\bar{s}(s)$, $\underline{w}_1(s)$ and $\overline{w}_1(s)$ all belong to $\mathscr{RL}_\infty$ and that $\underline{s}(s)$, $\bar{s}(s)$, $\underline{w}_1(s)$, $\overline{w}_1(s)$ are single-input single-output (SISO) transfer functions.

4.2.1. Maximizing the robust stability margin over W_1

The significance of the robust stability margin has earlier been stated in Section 3 and we now formulate this design objective that maximizes the robust stability margin (by minimizing γ) as follows:

$$b(P_s, C_\infty) := \left\| \begin{bmatrix} P_s \\ I \end{bmatrix} (I - C_\infty P_s)^{-1} \begin{bmatrix} -C_\infty & I \end{bmatrix} \right\|_\infty^{-1} > \frac{1}{\gamma}.$$

With some algebraic simplifications (Lanzon, 2005) and assuming $W_2 = I_m$, the above constraint can equivalently be written as

$$\begin{aligned}&\begin{bmatrix} 0 & P \\ 0 & I \end{bmatrix}^* \begin{bmatrix} I_m & 0 \\ 0 & \Lambda_{1\omega} \end{bmatrix} \begin{bmatrix} 0 & P \\ 0 & I \end{bmatrix} \\ &\quad < \gamma^2 \begin{bmatrix} I & P \\ \mathbf{C} & I \end{bmatrix}^* \begin{bmatrix} I_m & 0 \\ 0 & \Lambda_{1\omega} \end{bmatrix} \begin{bmatrix} I & P \\ \mathbf{C} & I \end{bmatrix}.\end{aligned} \tag{7}$$

Substituting $\Lambda_{1\omega}$ with $\mathbf{a}_p^{-1}B_p$ and multiplying both sides by $\mathbf{a}_p$ which is a positive scalar polynomial, (7) can be equivalently written as

$$\begin{bmatrix}0 & P\\ 0 & I\end{bmatrix}^*\begin{bmatrix}\mathbf{a}_pI_m & 0\\ 0 & B_p\end{bmatrix}\begin{bmatrix}0 & P\\ 0 & I\end{bmatrix} - \gamma^2\begin{bmatrix}I & P\\ \mathbf{C} & I\end{bmatrix}^*\begin{bmatrix}\mathbf{a}_pI_m & 0\\ 0 & B_p\end{bmatrix}\begin{bmatrix}I & P\\ \mathbf{C} & I\end{bmatrix} < 0. \tag{8}$$

Using expressions (4) and (6), constraint (8) can be represented as

$$\begin{bmatrix}0 & (I_m\otimes X)P\\ 0 & (I_n\otimes X)\end{bmatrix}^* M\begin{bmatrix}0 & (I_m\otimes X)P\\ 0 & (I_n\otimes X)\end{bmatrix} - \gamma^2\begin{bmatrix}(I_m\otimes X) & (I_m\otimes X)P\\ (I_n\otimes X)\mathbf{C} & (I_n\otimes X)\end{bmatrix}^* M\begin{bmatrix}(I_m\otimes X) & (I_m\otimes X)P\\ (I_n\otimes X)\mathbf{C} & (I_n\otimes X)\end{bmatrix} < 0, \tag{9}$$

where $M = \begin{bmatrix}I_m\otimes\bar{A}_p & 0\\ 0 & \bar{B}_p\end{bmatrix}$.

Inequality (9) can also be written as

$$\begin{bmatrix}0 & (I_m\otimes X)P\\ 0 & (I_n\otimes X)\\ (I_m\otimes X) & (I_m\otimes X)P\\ (I_n\otimes X)\mathbf{C} & (I_n\otimes X)\end{bmatrix}^*\begin{bmatrix}M & 0\\ 0 & -\gamma^2M\end{bmatrix} \times\begin{bmatrix}0 & (I_m\otimes X)P\\ 0 & (I_n\otimes X)\\ (I_m\otimes X) & (I_m\otimes X)P\\ (I_n\otimes X)\mathbf{C} & (I_n\otimes X)\end{bmatrix} < 0. \tag{10}$$

For a given P and $\mathbf{C}$, let (A_1, B_1, C_1, D_1) be a minimal state-space realization such that

$$\frac{1}{\alpha(s)}\begin{bmatrix}0 & (I_m\otimes X(s))P(s)\\ 0 & (I_n\otimes X(s))\\ (I_m\otimes X(s)) & (I_m\otimes X(s))P(s)\\ (I_n\otimes X(s))\mathbf{C}(s) & (I_n\otimes X(s))\end{bmatrix} = C_1(sI-A_1)^{-1}B_1 + D_1, \tag{11}$$

where $\alpha(s)$ is any p-th order polynomial with no root on the imaginary axis. Now, dividing (10) by $\alpha(j\omega)^*\alpha(j\omega)$, this constraint can then be equivalently expressed as

$$\begin{bmatrix}(j\omega I-A_1)^{-1}B_1\\ I\end{bmatrix}^*\begin{bmatrix}C_1 & D_1\end{bmatrix}^*\begin{bmatrix}M & 0\\ 0 & -\gamma^2M\end{bmatrix} \times\begin{bmatrix}C_1 & D_1\end{bmatrix}\begin{bmatrix}(j\omega I-A_1)^{-1}B_1\\ I\end{bmatrix} < 0 \quad \forall\omega. \tag{12}$$

Invoking the KYP lemma (Rantzer, 1996), inequality (12) is equivalent to the existence of a symmetric matrix $Q_1 \in \mathbb{R}^{n_1\times n_1}$ such that the following LMI holds

$$\begin{bmatrix}A_1^TQ_1+Q_1A_1 & Q_1B_1\\ B_1^TQ_1 & 0\end{bmatrix} + \begin{bmatrix}C_1 & D_1\end{bmatrix}^*\begin{bmatrix}M & 0\\ 0 & -\gamma^2M\end{bmatrix}\begin{bmatrix}C_1 & D_1\end{bmatrix} < 0. \tag{13}$$

Partitioning $C_1 = \begin{bmatrix}C_{11}\\ \hline C_{12}\end{bmatrix}$ and $D_1 = \begin{bmatrix}D_{11}\\ \hline D_{12}\end{bmatrix}$, where the dimensions of the partitioned matrices are compatible with M, we can write (13) in the form

$$\begin{bmatrix}A_1^TQ_1+Q_1A_1 & Q_1B_1\\ B_1^TQ_1 & 0\end{bmatrix} + \begin{bmatrix}C_{11} & D_{11}\end{bmatrix}^*M\begin{bmatrix}C_{11} & D_{11}\end{bmatrix} < \gamma^2\begin{bmatrix}C_{12} & D_{12}\end{bmatrix}^*M\begin{bmatrix}C_{12} & D_{12}\end{bmatrix}. \tag{14}$$

Constraint (14) can be posed as a generalized eigenvalue problem (GEVP) (Boyd, El Ghaoui, Feron, & Balakrishnan, 1994) since

$M > 0$ and

$$\begin{bmatrix}C_{12} & D_{12}\end{bmatrix} \neq 0 \Leftrightarrow \begin{bmatrix}C_{12} & D_{12}\end{bmatrix}^*M\begin{bmatrix}C_{12} & D_{12}\end{bmatrix} > 0.$$

In view of the objective to maximize the robust stability margin, γ^2 is the objective function while Q_1 and M (i.e., $\bar{A}_p$ and $\bar{B}_p$) are the decision variables in this quasiconvex optimization constraint.

4.2.2. Constraints for performance

Next, we formulate constraints (2a) which directly ensure that the desired performance specifications are met by restricting the singular values of the shaped plant within the pre-specified loop-shape boundaries $\underline{s}$ and $\bar{s}$ that characterize these specifications: $|\underline{s}| < \sigma_l(P_s(j\omega)) < |\bar{s}|\ \forall l$.

Substituting $P_s = PW_1$ since $W_2 = I_m$, the above can be expressed as $|\underline{s}|^2\Lambda_{1\omega} < P^*P < |\bar{s}|^2\Lambda_{1\omega}$.

Now, replace $\Lambda_{1\omega}$ with $\mathbf{a}_p^{-1}B_p$ in the above expression and multiply by $\mathbf{a}_p$:

$$|\underline{s}|^2B_p < \mathbf{a}_pP^*P < |\bar{s}|^2B_p.$$

Using the expressions in (5) and (6), and performing several algebraic manipulations similar to the previous formulation, the above constraints, invoking the KYP lemma, are equivalent to the existence of symmetric matrices $Q_2 \in \mathbb{R}^{n_2\times n_2}$ and $Q_3 \in \mathbb{R}^{n_3\times n_3}$ such that the following LMIs hold

$$\begin{bmatrix}A_2^TQ_2+Q_2A_2 & Q_2B_2\\ B_2^TQ_2 & 0\end{bmatrix} + \begin{bmatrix}C_2 & D_2\end{bmatrix}^*\begin{bmatrix}\bar{B}_p & 0\\ 0 & -I_m\otimes\bar{A}_p\end{bmatrix}\begin{bmatrix}C_2 & D_2\end{bmatrix} < 0, \tag{15}$$

$$\begin{bmatrix}A_3^TQ_3+Q_3A_3 & Q_3B_3\\ B_3^TQ_3 & 0\end{bmatrix} + \begin{bmatrix}C_3 & D_3\end{bmatrix}^*\begin{bmatrix}-\bar{B}_p & 0\\ 0 & I_m\otimes\bar{A}_p\end{bmatrix}\begin{bmatrix}C_3 & D_3\end{bmatrix} < 0. \tag{16}$$

Note that (A_2, B_2, C_2, D_2) and (A_3, B_3, C_3, D_3) in (15) and (16) are respectively minimal state-space realizations such that

$$\frac{1}{\alpha(s)}\begin{bmatrix}I_n\otimes\underline{s}(s)X(s)\\ P(s)\otimes X(s)\end{bmatrix} = C_2(sI-A_2)^{-1}B_2 + D_2, \tag{17a}$$

$$\frac{1}{\alpha(s)}\begin{bmatrix}I_n\otimes\bar{s}(s)X(s)\\ P(s)\otimes X(s)\end{bmatrix} = C_3(sI-A_3)^{-1}B_3 + D_3. \tag{17b}$$

Constraint (15) (resp. (16)) is simultaneously convex in its decision variables $\bar{A}_p$, $\bar{B}_p$ and Q_2 (resp. Q_3).

4.2.3. Constraints on the singular values of W_1

Since a designer needs to ensure that the singular values of the loop-shaping weights are within acceptable bounds, we also consider the constraints on the singular values of W_1 given in (2b) as follows:

$$|\underline{w}_1| < \sigma_l(W_1(j\omega)) < |\overline{w}_1| \quad \forall l \Leftrightarrow |\underline{w}_1|^{-2}I_n > \Lambda_{1\omega} > |\overline{w}_1|^{-2}I_n.$$

Replacing $\Lambda_{1\omega}$ with $\mathbf{a}_p^{-1}B_p$ in the above expression, we can then write

$$|\underline{w}_1|^{-2}I_n > \mathbf{a}_p^{-1}B_p > |\overline{w}_1|^{-2}I_n$$

$$\Leftrightarrow \mathbf{a}_p|\underline{w}_1|^{-2}I_n > B_p > \mathbf{a}_p|\overline{w}_1|^{-2}I_n.$$

Similarly, using (4) and (6) and performing some algebraic manipulations, these inequalities, invoking the KYP lemma, are

equivalent to the existence of symmetric matrices $Q_4 \in \mathbb{R}^{n_4\times n_4}$ and $Q_5 \in \mathbb{R}^{n_5\times n_5}$ such that the following LMIs hold:

$$\begin{bmatrix} A_4^TQ_4 + Q_4A_4 & Q_4B_4 \\ B_4^TQ_4 & 0 \end{bmatrix} + \begin{bmatrix} C_4 & D_4 \end{bmatrix}^* \begin{bmatrix} \bar{B}_p & 0 \\ 0 & -I_n \otimes \bar{A}_p \end{bmatrix} \begin{bmatrix} C_4 & D_4 \end{bmatrix} < 0, \tag{18}$$

$$\begin{bmatrix} A_5^TQ_5 + Q_5A_5 & Q_5B_5 \\ B_5^TQ_5 & 0 \end{bmatrix} + \begin{bmatrix} C_5 & D_5 \end{bmatrix}^* \begin{bmatrix} -\bar{B}_p & 0 \\ 0 & I_n \otimes \bar{A}_p \end{bmatrix} \begin{bmatrix} C_5 & D_5 \end{bmatrix} < 0. \tag{19}$$

Here, (A_4, B_4, C_4, D_4) and (A_5, B_5, C_5, D_5) are minimal state-space realizations such that

$$\frac{1}{\alpha(s)} \begin{bmatrix} I_n \otimes \underline{w}_2(s)X(s) \\ I_n \otimes X(s) \end{bmatrix} = C_4 (sI - A_4)^{-1} B_4 + D_4, \tag{20a}$$

$$\frac{1}{\alpha(s)} \begin{bmatrix} I_n \otimes \overline{w}_1(s)X(s) \\ I_n \otimes X(s) \end{bmatrix} = C_5 (sI - A_5)^{-1} B_5 + D_5. \tag{20b}$$

4.2.4. Constraint for the positivity of $\mathbf{a}_p$ and B_p

Finally, $\mathbf{a}_p$ and B_p are restricted to be positive in order to ensure that W_1 belongs to $\mathscr{GH}_\infty$. These constraints are cast in LMI framework as follows.

$$\mathbf{a}_p = X^*\bar{A}_pX > 0, \tag{21}$$

$$B_p = (I_n \otimes X)^* \bar{B}_p (I_n \otimes X) > 0. \tag{22}$$

If we divide both inequalities (21) and (22) by $\alpha(j\omega)^*\alpha(j\omega)$ each, and suppose also, minimal state-space realizations (A_6, B_6, C_6, D_6) and (A_7, B_7, C_7, D_7) such that

$$\frac{X(s)}{\alpha(s)} = C_6 (sI - A_6)^{-1} B_6 + D_6, \tag{23}$$

$$\frac{I_n \otimes X(s)}{\alpha(s)} = C_7 (sI - A_7)^{-1} B_7 + D_7, \tag{24}$$

constraints (21) and (22) can then be respectively written as

$$\begin{bmatrix} (j\omega I - A_6)^{-1} B_6 \\ I \end{bmatrix}^* \begin{bmatrix} C_6 & D_6 \end{bmatrix}^* \bar{A}_p \times \begin{bmatrix} C_6 & D_6 \end{bmatrix} \begin{bmatrix} (j\omega I - A_6)^{-1} B_6 \\ I \end{bmatrix} > 0 \quad \forall\omega, \tag{25}$$

$$\begin{bmatrix} (j\omega I - A_7)^{-1} B_7 \\ I \end{bmatrix}^* \begin{bmatrix} C_7 & D_7 \end{bmatrix}^* \bar{B}_p \times \begin{bmatrix} C_7 & D_7 \end{bmatrix} \begin{bmatrix} (j\omega I - A_7)^{-1} B_7 \\ I \end{bmatrix} > 0 \quad \forall\omega. \tag{26}$$

Invoking the KYP lemma, inequalities (25) and (26) are equivalent to the existence of symmetric matrices $Q_6 \in \mathbb{R}^{n_6\times n_6}$ and $Q_7 \in \mathbb{R}^{n_7\times n_7}$ such that the following LMIs hold

$$\begin{bmatrix} A_6^TQ_6 + Q_6A_6 & Q_6B_6 \\ B_6^TQ_6 & 0 \end{bmatrix} - \begin{bmatrix} C_6 & D_6 \end{bmatrix}^* \bar{A}_p \begin{bmatrix} C_6 & D_6 \end{bmatrix} < 0,$$

$$\begin{bmatrix} A_7^TQ_7 + Q_7A_7 & Q_7B_7 \\ B_7^TQ_7 & 0 \end{bmatrix} - \begin{bmatrix} C_7 & D_7 \end{bmatrix}^* \bar{B}_p \begin{bmatrix} C_7 & D_7 \end{bmatrix} < 0.$$

Remark 1. An identical $\alpha(s)$ can be used in the construction of the minimal state-space realizations (11), (17a), (17b), (20a), (20b), (23) and (24) without any loss of generalization. The only requirement is that the p-th order $\alpha(s)$ must not have any root on the imaginary axis.

4.3. Proposed optimization problem

In order to give the weight optimization problem in state-space characterization, we combine the formulation in the previous subsections as follows:

minimize γ^2

such that $\exists \mathbf{C} \in \mathscr{C}(P)$, $Q_i \in \mathbb{R}^{n_i\times n_i}$ $\forall i = 1, 2, \ldots, 7$

satisfying

$$\begin{bmatrix} A_1^TQ_1 + Q_1A_1 & Q_1B_1 \\ B_1^TQ_1 & 0 \end{bmatrix} + \begin{bmatrix} C_{11} & D_{11} \end{bmatrix}^* \begin{bmatrix} I \otimes \bar{A}_p & 0 \\ 0 & \bar{B}_p \end{bmatrix} \begin{bmatrix} C_{11} & D_{11} \end{bmatrix} < \gamma^2 \begin{bmatrix} C_{12} & D_{12} \end{bmatrix}^* \begin{bmatrix} I \otimes \bar{A}_p & 0 \\ 0 & \bar{B}_p \end{bmatrix} \begin{bmatrix} C_{12} & D_{12} \end{bmatrix}, \tag{27a}$$

$$\begin{bmatrix} A_2^TQ_2 + Q_2A_2 & Q_2B_2 \\ B_2^TQ_2 & 0 \end{bmatrix} + \begin{bmatrix} C_2 & D_2 \end{bmatrix}^* \begin{bmatrix} \bar{B}_p & 0 \\ 0 & -I \otimes \bar{A}_p \end{bmatrix} \begin{bmatrix} C_2 & D_2 \end{bmatrix} < 0, \tag{27b}$$

$$\begin{bmatrix} A_3^TQ_3 + Q_3A_3 & Q_3B_3 \\ B_3^TQ_3 & 0 \end{bmatrix} + \begin{bmatrix} C_3 & D_3 \end{bmatrix}^* \begin{bmatrix} -\bar{B}_p & 0 \\ 0 & I \otimes \bar{A}_p \end{bmatrix} \begin{bmatrix} C_3 & D_3 \end{bmatrix} < 0, \tag{27c}$$

$$\begin{bmatrix} A_4^TQ_4 + Q_4A_4 & Q_4B_4 \\ B_4^TQ_4 & 0 \end{bmatrix} + \begin{bmatrix} C_4 & D_4 \end{bmatrix}^* \begin{bmatrix} \bar{B}_p & 0 \\ 0 & -I \otimes \bar{A}_p \end{bmatrix} \begin{bmatrix} C_4 & D_4 \end{bmatrix} < 0, \tag{27d}$$

$$\begin{bmatrix} A_5^TQ_5 + Q_5A_5 & Q_5B_5 \\ B_5^TQ_5 & 0 \end{bmatrix} + \begin{bmatrix} C_5 & D_5 \end{bmatrix}^* \begin{bmatrix} -\bar{B}_p & 0 \\ 0 & I \otimes \bar{A}_p \end{bmatrix} \begin{bmatrix} C_5 & D_5 \end{bmatrix} < 0, \tag{27e}$$

$$\begin{bmatrix} A_6^TQ_6 + Q_6A_6 & Q_6B_6 \\ B_6^TQ_6 & 0 \end{bmatrix} - \begin{bmatrix} C_6 & D_6 \end{bmatrix}^* \bar{A}_p \begin{bmatrix} C_6 & D_6 \end{bmatrix} < 0, \tag{27f}$$

$$\begin{bmatrix} A_7^TQ_7 + Q_7A_7 & Q_7B_7 \\ B_7^TQ_7 & 0 \end{bmatrix} - \begin{bmatrix} C_7 & D_7 \end{bmatrix}^* \bar{B}_p \begin{bmatrix} C_7 & D_7 \end{bmatrix} < 0, \tag{27g}$$

where (A_i, B_i, C_i, D_i), $i = 1, 2, \ldots, 7$ are minimal state-space realizations of (11), (17a), (17b), (20a), (20b), (23) and (24), respectively. Symmetric matrices $Q_i \in \mathbb{R}^{n_i\times n_i}$ $(i = 1, 2, \ldots, 7)$, $\bar{A}_p$ and $\bar{B}_p$ are the decision variables in the optimization problem. The optimization problem is quasiconvex when the stabilizing controller $\mathbf{C} \in \mathscr{C}(P)$ is held fixed in (11) and can be easily solved using LMI routines, for example, '*gevp*' solver in MATLAB LMI toolbox.

In this optimization problem that is over a fixed-order bi-proper pre-compensator, inequality (27a) captures the cost function that maximizes the robust stability margin $b(P_s, C_\infty)$ while (27b)–(27c) delimit the singular values of the shaped plant P_s within the specified loop-shape boundaries $\underline{s}(s)$ and $\bar{s}(s)$ that capture performance specifications. In addition, (27d)–(27e) provide bounds on the singular values of the synthesized pre-compensator while (27f) and (27g) respectively enforce the positivity of $\bar{A}_p$ and $\bar{B}_p$ in order to guarantee that the synthesized weight belongs to $\mathscr{GH}_\infty$. We have considered diagonal weight in this formulation, but with slight modification in the parameterizations of the weight as implemented in Sandberg et al. (2006a,b), it is easy to extend the formulation for non-diagonal weight synthesis while still retaining the quasiconvexity of the optimization problem.

Remark 2. Constraint on the condition number of W_1 in (2c) has not been directly addressed in the foregoing formulation.

Note that two of the standard closed-loop design objectives are specified as function of the condition number of W_1 (McFarlane & Glover, 1990; Zhou et al., 1996): the gain from plant input disturbance to controller output ($\overline{\sigma}(\mathbf{C}(I + P\mathbf{C})^{-1}P) \leq \min\{\gamma\overline{\sigma}(\tilde{N}_s)\kappa(W_1), 1 + \gamma\overline{\sigma}(M_s)\kappa(W_1)\}$) and the gain from plant output disturbance to error signal ($\overline{\sigma}((I + \mathbf{C}P)^{-1}) \leq \min\{1 + \gamma\overline{\sigma}(\tilde{N}_s)\kappa(W_1), \gamma\overline{\sigma}(M_s)\kappa(W_1)\}$), both of which should be made small, typically at low frequencies. In the above expressions, the pair $(\tilde{N}_s, \tilde{M}_s)$ (resp. (N_s, M_s)) $\in \mathscr{RH}_\infty$ constitute a normalized left (resp. right) coprime factorization of P_s (McFarlane & Glover, 1992). At low frequencies, $\underline{\sigma}(P_s)$ is typically large. Hence, $\overline{\sigma}(M_s) = \left[\frac{1}{1+\overline{\sigma}(P_s)^2}\right]^{1/2}$ is small, which implies that $1 + \gamma\overline{\sigma}(M_s)\kappa(W_1)$ and $\gamma\overline{\sigma}(M_s)\kappa(W_1)$ are made small at these frequencies. Constraint on the condition number of W_1 can therefore be relaxed. However, the choice of $\underline{w}_1(s)$ and $\overline{w}_1(s)$ can be made to indirectly ensure that the condition number of W_1 is bounded, especially at low frequencies, i.e., for a given $\underline{w}_1(s)$ and $\overline{w}_1(s)$ that satisfies $\frac{|\overline{w}_1(j\omega)|}{|\underline{w}_1(j\omega)|} < k_1$, then $\kappa(W_1(j\omega)) < k_1$.

$$\left(\overline{\sigma}(W_1) < |\overline{w}_1|, \underline{\sigma}(W_1) > |\underline{w}_1| \Rightarrow \frac{\overline{\sigma}(W_1)}{\underline{\sigma}(W_1)} < k_1 \Leftrightarrow \kappa(W_1) < k_1.\right)$$

5. Solution algorithm

A sub-optimal solution algorithm is now proposed based on the state-space formulation given in the previous section. Similar to solution methods for these types of optimization problems (Lanzon & Cantoni, 2003; Lanzon & Tsiotras, 2005; Zhou et al., 1996), for instance, *D-K* iterations, the posed problem must be solved iteratively since it is not simultaneously convex in the controller C and the parameters of the pre-compensator W_1 ($\bar{A}_p$ and $\bar{B}_p$), used in the construction of the respective minimal state-space realizations.

Inputs to the algorithm.

- A scaled nominal plant P.
- Transfer functions $\underline{s}(s)$ and $\bar{s}(s)$ that are boundaries for an allowable loop-shape.
- Transfer functions $\underline{w}_1(s)$ and $\overline{w}_1(s)$ that delimit the allowable region for the singular values of W_1.
- A positive integer p that specifies the desired order of W_1.

The solution algorithm.

(1) As a feasible initial starting point for the algorithm, find a controller $\mathbf{C}_0^\star$ such that $\left[P, \mathbf{C}_0^\star\right]$ is internally stable. Set $i = 0$, where i denotes the iteration number and let $\varepsilon^\star_{\max,0} = -1$.
(2) Increment i by 1.
(3) Formulate and solve the quasiconvex[3] optimization problem in Section 4.3. Denote by $\bar{A}_p^\star$ and $\bar{B}_p^\star$ the values of $\bar{A}_p$ and $\bar{B}_p$ that achieve the minimum γ_i^{2} (denoted by $\gamma_i^{2^\star}$) of the optimization problem. Furthermore, form $\Lambda^\star_{1\omega} = \mathbf{a}_p(\omega^2)^{-1}B_p(\omega^2)$ using the values of $\bar{A}_p^\star$ and $\bar{B}_p^\star$.
(4) Compute a spectral factorization of $\Lambda^\star_{1\omega}$ such that $W^{\star}_{1,i}{}^{\sim}W^\star_{1,i} = \Lambda^{\star^{-1}}_{1\omega}$ and $W^\star_{1,i} \in \mathscr{GH}_\infty$.
(5) Compute $b_{opt}(PW^\star_{1,i})$ as detailed in Glover and McFarlane (1989) and let this value be denoted by $\varepsilon^\star_{\max,i}$. Furthermore, synthesize a controller $C^\star_{\infty,i}$ that achieves a robust stability margin $b(PW^\star_{1,i}, C^\star_{\infty,i}) = \varepsilon^\star_{\max,i}$ usually using the state-space formula given in Glover (1984, Theorem 6.3). Set $\mathbf{C}_i^\star = W^\star_{1,i}C^\star_{\infty,i}$.
(6) Evaluate $(\varepsilon^\star_{\max,i} - \varepsilon^\star_{\max,i-1})$. If this difference (which is always positive) is very small, for instance 0.01, and has remained this small for the last few iterations, then EXIT; otherwise return to Step 2.

Outputs of the algorithm.

- The maximized value of $b_{opt}(P_s)$ obtained in the variable $\varepsilon^\star_{\max,i}$.
- A diagonal loop-shaping weight $W^\star_{1,i}$ that achieves $\varepsilon^\star_{\max,i}$.
- A controller $C^\star_{\infty,i}(s)$ that achieves $b(PW^\star_{1,i}, C^\star_{\infty,i}) = \varepsilon^\star_{\max,i}$.

Remark 3. (1) Being an ascent algorithm, the value of $\varepsilon^\star_{\max,i}$ is monotonically non-decreasing as i increases (due to the existence of weight(s), for instance, $W^\star_{1,i} = I$, such that $b(PW^\star_{1,i}, W^{\star^{-1}}_{1,i-1}C^\star_{i-1}) \geq \varepsilon^\star_{\max,i-1}$) and at each iteration, $\sqrt{\frac{1}{\gamma_i^{2^\star}}} \geq \varepsilon^\star_{\max,i-1}$. Note that the algorithm cannot however guarantee convergence to the global minimum; only monotonicity properties can be guaranteed. The use of the algorithm on various practical design examples has however shown that it is quite insensitive to the initial choice of a stabilizing controller $\mathbf{C}_0^\star$ and this is most probably due to the fact that it has enough freedom to rectify a poor choice of initial stabilizing controller at both optimization Steps 3 (via W_1) and 5 (via C_∞) of each iteration.
(2) Should any of the constraints (27a)–(27g) be required to only hold within a finite frequency range, the finite frequency KYP lemma (Graham, Oliveira, & de Callafon, 2009; Iwasaki, Meinsma, & Fu, 2000) can be invoked in lieu of the KYP lemma Rantzer (1996). Then, the convex constraint will hold accordingly for all frequency $|\omega| \leq \omega_0, \omega_0 \in \mathbb{R}_+$ or $\omega_1 \leq \omega \leq \omega_2$, where ω_1 and ω_2 are the required lower and upper frequency bounds, respectively.

6. Numerical example

The following numerical examples illustrate the effectiveness of the solution algorithm proposed in the previous section. The algorithm has been coded in MATLAB 7.3 on a 2.66 GHz Intel® Core™ 2 PC.

Example 1. We consider a lightly-damped (damping ratio of 0.02) SISO plant with poles and zeros at $s = -0.0283 \pm j1.4139$, $-1.5 \pm j1.6583$ and $s = -0.4 \pm j19.996$, respectively. The transfer function of the nominal plant is given below and its magnitude plot is shown in Fig. 2.

$$P = \frac{10\left(s^2 + 0.8s + 400\right)}{\left(s^2 + 0.0566s + 2\right)\left(s^2 + 3s + 5\right)}.$$

Based on the desired closed-loop design objectives, for instance, low frequency gain indicating disturbance rejection and reference signal tracking, bandwidth and roll-off rate around crossover frequency indicating stability and damping, high frequency gain indicating insensitivity to sensor-noise and unmodeled dynamics, etc., the loop-shape boundaries are selected as

$$\underline{s}(s) = \frac{10^3\left(\frac{s}{0.3} + 1\right)\left(s^2 + 1.1 \times 10^4 s + 4.65 \times 10^7\right)}{\left(\frac{s}{0.03} + 1\right)^2\left(\frac{s}{30} + 1\right)^7};$$

$$\bar{s}(s) = \frac{10^5\left(\frac{s}{2} + 1\right)^4}{\left(\frac{s}{0.2} + 1\right)^4\left(\frac{s}{200} + 1\right)^3}.$$

Firstly, we exemplify the problems associated with frequency gridding by using the solution algorithm to the pointwise-in-frequency weight optimization problem stated in Section 3. Frequency functions $|\underline{w}_1(j\omega)|$ and $|\overline{w}_1(j\omega)|$ that confine the singular values of W_1 are chosen as 10^{-2} and 10^2, respectively, and the frequency space between $\omega = 10^{-5}$ and 10^5 rad/s is divided

[3] For constraint (27a) in Section 4.3, $\mathbf{C}^\star_{i-1}$ is used to obtain the minimal realization of (A_1, B_1, C_1, D_1) at the i-th iteration.

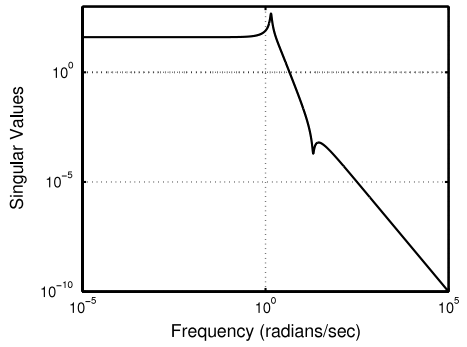

Fig. 2. Magnitude plot of the nominal plant P.

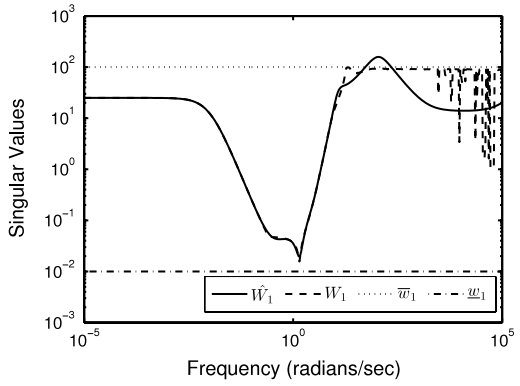

Fig. 3. Curve-fitting using the pointwise-in-frequency weight optimization problem: $\hat{W}_1$ is the fitted transfer function while W_1 is the obtained magnitude data.

into 500 grid-points. The difficulty in curve-fitting is shown in Fig. 3, where an 11-th order transfer function is fitted to the magnitude data obtained as solution to the optimization problem at the first iteration. There is some considerable inaccuracies in fitting at high frequencies as depicted in the figure. It should be noted that higher-order transfer functions did not improve the accuracy of the curve-fitting. Furthermore, it is observed that the singular values of the synthesized weight do not lie entirely within the specified region due to an inaccurate curve-fitting, i.e., constraints on the singular values of the pre-compensator are violated at certain frequencies, which is undesirable.

Now, the solution algorithm proposed in Section 5 is used to simultaneously synthesize a pre-compensator W_1 and a stabilizing controller C_∞ that maximize the robust stability margin for the given performance. Since the condition number of SISO system is always 1, the transfer functions $\underline{w}_1(s)$ and $\overline{w}_1(s)$, capturing the bounds on the singular values of the weight, are chosen as gains 10^{-1} and 10^2, respectively. The order p of the weight is fixed 'a priori' as 3. Note that these choices always depend on the particular problem and hence, a different design specification might require designers to select more complicated bounds and/or higher order for the weight. The solution algorithm is now invoked and it practically converges after three iterations. The singular values of the synthesized pre-compensator W_1, the correspondingly achieved loop-shape P_s and the singular values of the simultaneously synthesized controller C_∞ are shown in Fig. 4.

Performance specifications are met in the cascade formed between the nominal plant and the synthesized compensator since the resulting loop-shape lies within the pre-specified region. It is interesting to note that the lightly-damped poles and zeros of the nominal plant are retained in the shaped plant because the synthesized compensator has smooth magnitude response. An otherwise lightly-damped pole-zero cancellation is not desirable as this affects the robust performance and robust stability of the closed-loop system (see Osinuga, Patra, & Lanzon, 2010). The robust stability margin of 0.4098 is obtained and the order of the synthesized robust stabilizing controller C_∞ is 6. The synthesized weight W_1 is given in state-space representation below:

$$\left[\begin{array}{ccc|c} -21.7673 & 30.2170 & 0 & 0.2402 \\ -23.6151 & -31.3001 & 0 & 7.9331 \\ -0.0039 & -0.0278 & -0.0028 & -0.0013 \\ \hline -132.9478 & -625.4162 & -24.2412 & 98.6521 \end{array}\right].$$

Example 2. The second example used to demonstrate the applicability of the proposed algorithm is MIMO system taken from process control literature (Loh, Hang, Quek, & Vasnani, 1993), which consists of a 24-tray tower separating methanol and water. The transfer function model for controlling the temperature t on the 4-th (stripping section) and 17-th (rectifying section) trays is given as

$$\begin{bmatrix} t_{17} \\ t_4 \end{bmatrix} = \begin{bmatrix} \dfrac{-2.2e^{-s}}{7s+1} & \dfrac{1.3e^{-0.3s}}{7s+1} \\ \dfrac{-2.8e^{-1.8s}}{9.5s+1} & \dfrac{4.3e^{-0.35s}}{9.2s+1} \end{bmatrix} \begin{bmatrix} r \\ s \end{bmatrix},$$

where the manipulated variables are reflux r and steam-flow s; the singular values are shown in Fig. 5. Since the time delays are moderate, they are realized by their 2nd order Padé approximations. Here, the objective is to achieve a unity crossover frequency of approximately 2 rad/s and a good reference signal tracking, i.e., maximized loop-gain at low frequencies. These specifications are approximately captured within the loop-shape boundaries

$$\underline{s}(s) = \frac{2.8 \times 10^7}{(s+0.02)\,(s+80)^4}; \qquad \overline{s}(s) = \frac{4.6 \times 10^2}{(s+0.009)\,(s+40)}.$$

Since the pre-compensator cannot roll-off at high frequencies as it is always a bi-proper transfer function, desired roll-off is realized by cascading a low-pass filter with corner frequency of 30 rad/s with the nominal plant. The transfer functions $\underline{w}_1(s)$ and $\overline{w}_1(s)$ that confine the singular values of W_1 are chosen as gains of 6.5 and 40, respectively, while the order p of W_1 is simply chosen as 2 in order to facilitate the synthesis of a low-order controller. The proposed solution algorithm, where performance related constraints (27b) and (27c) are structured to only hold for all frequencies $|\omega| \leq 10^3$ rad/s by invoking the finite frequency lemma (Iwasaki et al., 2000), is then used to simultaneously synthesize W_1 and C_∞.

Accordingly, the singular values of W_1, P_s and C_∞ at the end of the third iteration when the solution algorithm has practically converged are shown in Fig. 5. It is obvious that the shaped plant lies within the pre-specified loop-shape boundaries, selected based on performance objectives, thus implying that the desired performance specifications are satisfied. The condition number of W_1 is less than 1.3 at all frequencies, which is typically considered good. Finally, and of huge significance, the robust stability margin of 0.3511 is obtained, which is an indicator of a decent design. The order of the synthesized robust stabilizing controller C_∞ is 14 states and this can be reduced using model reduction techniques given in Zhou et al. (1996), if required. The synthesized weight is given in state-space representation below:

$$\left[\begin{array}{cc|cc} -0.0687 & 0 & 2 & 0 \\ 0 & -0.0760 & 0 & 1 \\ \hline 1.0978 & 0 & 7.1949 & 0 \\ 0 & 1.9573 & 0 & 6.5702 \end{array}\right].$$

The unit step responses of the system with the corresponding control signals are respectively shown in the last two plots in Fig. 5, where the closed-loop performance is seen to be satisfactory.

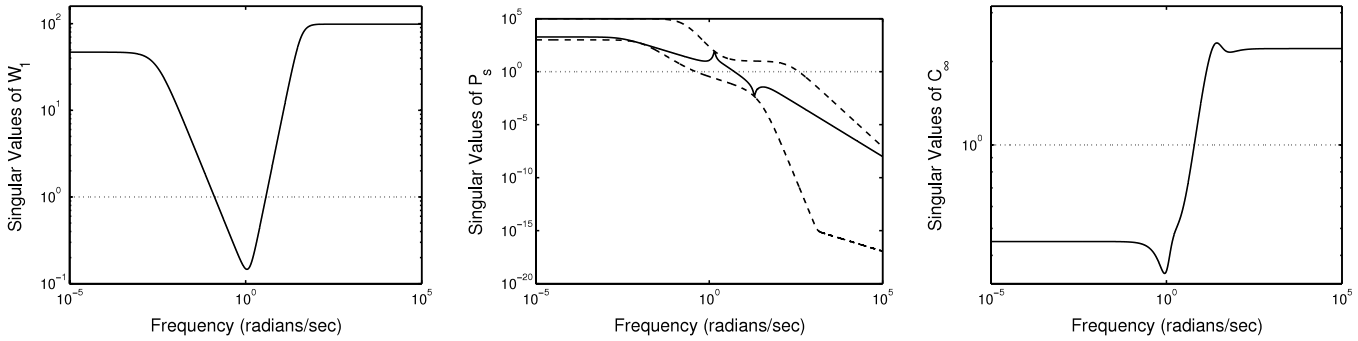

Fig. 4. Singular value plots for W_1, P_s and C_∞.

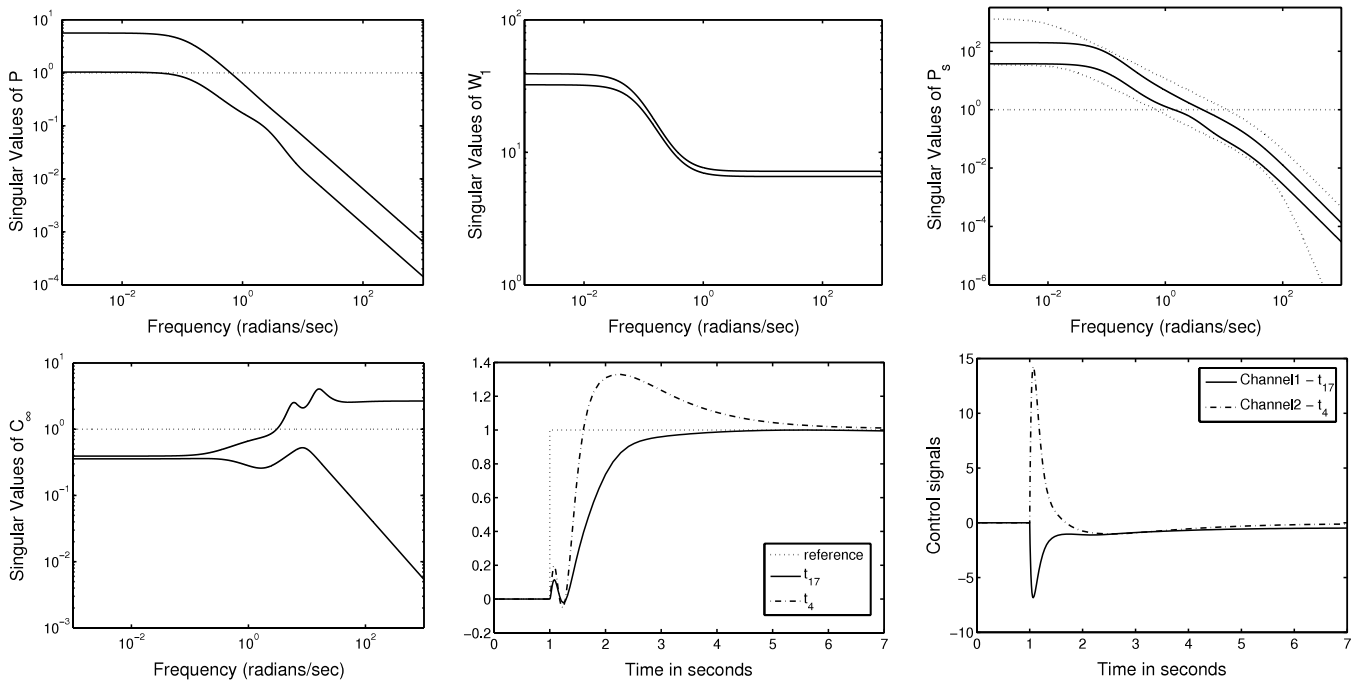

Fig. 5. Singular value plots for P, W_1, P_s, C_∞ and unit step responses (reflux and steam flow) of the MIMO system and the control signal.

Example 3. The same example used in Lanzon (2005) is now considered (see the paper for more details). Choosing the order of the pre-compensator as $p = 2$ and using the same specifications given in the above paper, the resulting weight from the proposed state-space algorithm is given as $W_1 = \left(\begin{array}{c|c} A_{W_1} & B_{W_1} \\ \hline C_{W_1} & D_{W_1} \end{array}\right)$, where

$$A_{W_1} = \begin{pmatrix} -0.003 & -1.4594 & 0 & 0 \\ 1.4594 & -748.597 & 0 & 0 \\ 0 & 0 & -0.0021 & -1.5631 \\ 0 & 0 & 1.5631 & -479.7979 \end{pmatrix},$$

$$B_{W_1} = \begin{pmatrix} -10.6547 & 2190.7 & 0 & 0 \\ 0 & 0 & -7.5884 & 1948.7 \end{pmatrix}^T,$$

$$C_{W_1} = \begin{pmatrix} -10.6547 & -2190.7 & 0 & 0 \\ 0 & 0 & -7.5884 & -1948.7 \end{pmatrix}$$

and

$$D_{W_1} = \begin{pmatrix} 6419 & 0 \\ 0 & 7941 \end{pmatrix}.$$

The singular values of this weight and the correspondingly achieved loop-shape are shown in Fig. 6. We obtain a $b(P_s, C_\infty)$ of 0.3315, which is satisfactory and comparable to the $b(P_s, C_\infty)$ of 0.368 obtained in Lanzon (2005) where the pre-compensator had 8 states.

7. Conclusion

This work formulates a weight optimization problem that is dependent on frequency into a finite number of optimization constraints that are independent of frequency. The introduced optimization problem maximizes the robust stability margin over a fixed-order pre-compensator, thus facilitating the synthesis of low-order optimal controllers in $\mathscr{H}_\infty$ loop-shaping control. The steps of the standard $\mathscr{H}_\infty$ loop-shaping design procedure are combined in the proposed optimization framework. Consequently, the procedure simultaneously optimizes the robust performance and the robust stability of a closed-loop system in a systematic framework. The algorithm is computationally efficient as the optimization problem is formulated in a quasiconvex framework, which is easily implementable using the available LMI toolbox.

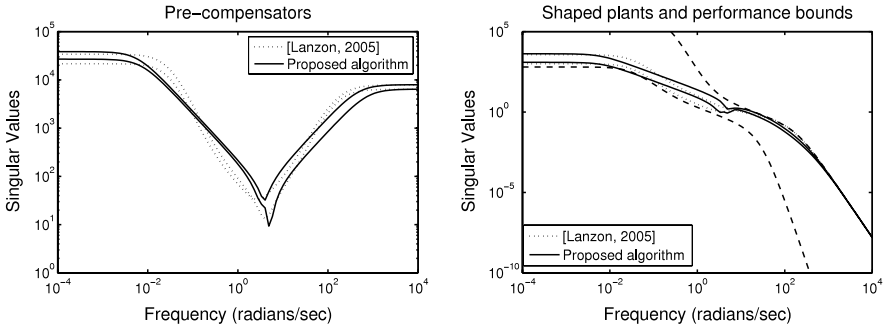

Fig. 6. Loop-shaping weight and shaped plant.

Acknowledgements

The authors would like to thank the Associate Editor and the anonymous reviewers for their useful comments.

References

Boyd, S., El Ghaoui, L., Feron, E., & Balakrishnan, V. (1994). *Linear matrix inequalities in system and control theory*: *Vol. 15*. Philadelphia: Society for Industrial and Applied Mathematics.

Glover, K. (1984). All optimal hankel-norm approximations of linear multivariable systems and their $\mathscr{L}_\infty$-error bounds. *International Journal of Control*, *39*(6), 1115–1193.

Glover, K., & McFarlane, D. (1989). Robust stabilization of normalized coprime factor plant descriptions with $\mathscr{H}_\infty$-bounded uncertainty. *IEEE Transactions on Automatic Control*, *34*(8), 821–830.

Graham, M., Oliveira, M., & de Callafon, R. (2009). An alternative Kalman–Yakubovich–Popov lemma and some extensions. *Automatica*, *45*(6), 1489–1496.

Hyde, R (1995). $\mathscr{H}_\infty$ aerospace control design-a VSTOL flight application. In *Advances in industrial control series*. Berlin: Springer.

Iwasaki, T., Meinsma, G., & Fu, M. (2000). Generalized *S*-procedure and finite frequency KYP lemma. *Mathematical Problems in Engineering*, *6*(2–3), 305–320.

Lanzon, A. (2001). Simultaneous synthesis of weights and controllers in $\mathscr{H}_\infty$ loop-shaping. In *Proceedings of IEEE conference on decision and control, Orlando, FL, US* (pp. 670–675).

Lanzon, A. (2005). Weight optimisation in $\mathscr{H}_\infty$ loop-shaping. *Automatica*, *41*(1), 1201–1208.

Lanzon, A., & Cantoni, M. (2003). On the formulation and solution of robust performance problems. *Automatica*, *39*(10), 1707–1720.

Lanzon, A., & Tsiotras, P. (2005). A combined application of $\mathscr{H}_\infty$ loop-shaping and μ-synthesis to control high-speed flywheels. *IEEE Transactions on Control Systems Technology*, *13*(5), 766–777.

Loh, A., Hang, C., Quek, K., & Vasnani, V. (1993). Autotuning of multiloop proportional-integral controllers using relay feedback. *Industrial & Engineering Chemistry Research*, *32*(6), 1102–1107.

McFarlane, D., & Glover, K. (1990). *Lecture notes in control and information sciences*: *Vol. 138*. *Robust controller design using normalized coprime factor plant descriptions*. Springer-Verlag.

McFarlane, D., & Glover, K. (1992). A loop-shaping design procedure using $\mathscr{H}_\infty$ synthesis. *IEEE Transactions on Automatic Control*, *37*(6), 759–769.

Osinuga, M., Patra, S., & Lanzon, A. (2010). Smooth weight optimization in $\mathscr{H}_\infty$ loop-shaping design. *Systems and Control Letters*, *59*, 663–670.

Papageorgiou, G., & Glover, K. (1997). A systematic procedure for designing non-diagonal weights to facilitate $\mathscr{H}_\infty$ loop shaping. In *Proceedings of IEEE conference on decision and control, San Diego, CA, US* (pp. 2127–2132).

Rantzer, A. (1996). On the Kalman–Yakubovich–Popov lemma. *Systems and Control Letters*, *28*(1), 7–10.

Sandberg, H., Lanzon, A., & Anderson, B. (2006a). Model approximation using magnitude and phase criteria: implications for model reduction and system identification. *International Journal of Robust and Nonlinear Control*, *17*(5–6), 435–461.

Sandberg, H., Lanzon, A., & Anderson, B. (2006b). Transfer function approximation and identification using magnitude and phase criteria. In *Proceedings of the 17th international symposium on mathematical theory of networks and systems, Kyoto, Japan* (pp. 250–256).

Tsai, M., Geddes, E., & Postlethwaite, I. (1990). Pole-zero cancellations and closed-loop properties of an $\mathscr{H}_\infty$ mixed sensitivity design problem. In *Proceedings of IEEE conference on decision and control, Honolulu, HI, USA* (pp. 1028–1029).

Vinnicombe, G. (2001). *Uncertainty and feedback: $\mathscr{H}_\infty$ loop-shaping and υ-gap metric*. Imperial College Press.

Zhou, K., Doyle, J., & Glover, K. (1996). *Robust and optimal control*. Englewood Cliffs, NJ: Prentice Hall.

Mobolaji Osinuga obtained a B.Sc. (Hons) degree in Electronic and Electrical Engineering at the Obafemi Awolowo University, Nigeria. With over 5 years of ample industrial experience in the field of telecommunication and systems integration, he proceeded to the University of Manchester in 2007, where he successfully completed his M.Sc. course in Advanced Control and Systems Engineering. He is currently a research student at the same institution, where he works on weight optimization in robust control and applications.

Sourav Patra received the Ph.D. degree in Electrical Engineering from Indian Institute of Technology Kharagpur, India in 2009. He is currently appointed as a lecturer at the Department of Electrical Engineering, Indian Institute of Technology, Kharagpur, India, having previously worked as a Postdoctoral Research Associate at the Control Systems Centre, School of Electrical and Electronic Engineering, University of Manchester, UK. Prior to this position, he was appointed as a Reader in the Department of Avionics, Indian Institute of Space Science and Technology Trivandrum, India. His major research area is robust control, and other research interests include the actuator saturator control, time-delay systems, nonlinear systems and systems biology.

Alexander Lanzon was born in Malta. He received the B.Eng.(Hons). degree in Electrical Engineering from the University of Malta in 1995, and his Masters' and Ph.D. degrees in Control Engineering from the University of Cambridge in 1997 and 2000, respectively. Before joining the University of Manchester in 2006, Dr Lanzon held academic positions at Georgia Institute of Technology and the Australian National University. Lanzon also received earlier research training at Bauman Moscow State Technical University, Russia, and industrial training at ST-Microelectronics Ltd., National ICT Australia Ltd. and Yaskawa Denki Tokyo Ltd, Japan. His research interests include fundamental theory of feedback systems, robust control and applications to aerospace control (including UAVs and control of new vehicle concepts). Dr Lanzon is a fellow of the IET, a senior member of IEEE and a member of AIAA.